

UDK 692.533.1; 546.261; 622.785

Microstructure and Thermal Properties of Cu-SiC Composite Materials Depending on the Sintering Technique

Marcin Chmielewski¹, Katarzyna Pietrzak¹, Agata Strojny-Nędzia^{1*},
Kamil Kaszyca¹, Rafał Zybala², Piotr Bazarnik², Małgorzata
Lewandowska², Szymon Nosewicz³

¹Institute of Electronic Materials Technology, 133 Wolczyńska Str, 01-919 Warsaw, Poland

²Faculty of Materials Science and Engineering, Warsaw University of Technology, 141 Wołoska Str, 02-507 Warsaw, Poland

³Institute of Fundamental Technological Research, Polish Academy of Sciences, 5B Pawińskiego Str, 02-106 Warsaw, Poland

Abstract:

The presented paper investigates the relationship between the microstructure and thermal properties of copper–silicon carbide composites obtained through hot pressing (HP) and spark plasma sintering (SPS) techniques. The microstructural analysis showed a better densification in the case of composites sintered in the SPS process. TEM investigations revealed the presence of silicon in the area of metallic matrix in the region close to metal-ceramic boundary. It is the product of silicon dissolving process in copper occurring at an elevated temperature. The Cu-SiC interface is significantly defected in composites obtained through the hot pressing method, which has a major influence on the thermal conductivity of materials.

Keywords: Metal matrix composites; Silicon carbide; Interface; Spark plasma sintering; Thermal conductivity.

1. Introduction

Among advanced structural materials, metal matrix composites (MMC's) play a significant role. For a practical application of metal-ceramic composites in electronic industry (e.g. as heat dissipation elements) the following requirements should be assured:

- a composite material should have a homogeneous structure and a high relative density (maximum reduction or elimination of porosity),
- the material should exhibit a high thermal conductivity (similar to that of copper) and, at the same time, the coefficient of linear thermal expansion should be kept relatively low,
- the bonding between the matrix and the ceramic reinforcement should be stable in a wide range of operation temperatures.

One of the fundamental issues in the field of metal-ceramic composites is the formation of matrix/reinforcement interfaces [1]. The structure of the interface which depends on a number

*) Corresponding author: agata.strojny@itme.edu.pl

of different factors may have a major effect on the properties of composites, comparable to that of the matrix and the reinforcing phase themselves. Apart from the most important conditions of the manufacturing process, such as temperature, pressure, time and atmosphere, also the following factors have a significant effect on the interface properties: the amount, form, shape, dimensions and distribution homogeneity of the reinforcement [2].

Materials intended for use in electronics as heat-dissipation elements (e.g. diodes, thyristors and lasers) should be characterized by the following features: a high thermal conductivity, the thermal expansion coefficient matched with the properties of semiconductor materials (Si, GaAs – $3.0\text{-}6.0 \times 10^{-6}$ 1/K), good mechanical properties, the ability to form durable joints, the stability of the structure during thermal cycles and a low cost [3].

There are many studies on the design and manufacturing of advanced materials characterized by a very good thermal conductivity, such as Cu-Mo, Cu-Be, Cu-C, Cu-SiC, Cu-AlN, Al-SiC, Al-AlN [4-10]. Having analyzed the characteristics of materials likely to have good thermal properties and the available scientific literature on the composite materials engineering, we have opted for the copper-silicon carbide pair as a material with great scientific and technological potential. Copper can be applied whenever a high thermal and electrical conductivity is required. The transport properties (heat or current transport) of copper depend mainly on its purity. Heat conductivity in the case of copper reaches around 400W/mK. However, a high coefficient of thermal expansion in the case of copper (16.5×10^{-6} 1/K) may be the reason of thermal residual stresses. Silicon carbide (SiC) is a semiconductor with a wide band gap E_g , the value of which ranges between 2.38 eV and 3.26 eV, depending on the polytype. Due to its unique physical and chemical properties such as high breakdown electric field, a high thermal and electric conductivity, a high hardness as well as heat and chemical resistance, SiC is a particularly attractive material applied to the manufacturing of high power/high frequency electronic devices working in high-temperature environments. The literature provides some information concerning the manufacturing techniques of the Cu-SiC composites. The hot-pressing method is used most frequently [6,11-12]. Authors of [13] reported that pulse spraying can be applied to obtain Cu-SiC composite layers.

It should be noticed that copper decomposes SiC to Si and C at an elevated temperature [14]. As a result of this process, silicon is dissolved into copper, which highly influences the decrease of thermal conductivity of the matrix. The affinity of C for Cu and the solubility of C in Cu are negligible [15]. Additionally, the remaining layer of carbon impedes good bonding at metal-ceramic interface [12].

Therefore, special attention should be given to the phenomena at the area of metal-ceramic boundary. The consolidation process should assure the maximum densification of the material, but without any structural changes in the interface area. That is why both techniques of sintering (hot-pressing and spark plasma sintering) have been selected to examine the influence of sintering conditions on the microstructure and thermal conductivity. The hot-pressing method is a conventional technique used for the consolidation of different kinds of powders (ceramic, metallic, composite). Diffusion is responsible for mass transport and determines the final material properties. Spark plasma sintering is influenced by a combination of both pressure and temperature, accompanied by the passage of electric current. The possibility of performing a quick pressing process of various powders has to be enumerated as its predominant advantage. Arcing can appear in pores during electric current assisted sintering, thus intensifying the sintering processes [16].

The objectives of the presented paper were: (i) to manufacture Cu-SiC metal matrix composite materials using the hot-pressing and spark plasma sintering method, (ii) to characterise the microstructure of composites with special attention to the ceramic-metal interface, and (iii) to find the correlation between the structure of material and its thermal conductivity.

2. Experimental procedure

Copper powder (with the average grain size of 40 μm , NewMet Koch) with a commercial purity of more than 99.99 % was used as the starting material for the metal matrix. Silicon carbide particles of a mean size of about 80 μm (product of Saint-Gobain), purity 99.99 %, was selected as the reinforcement phase. Fig. 1 shows microstructure of powders used for synthesis.

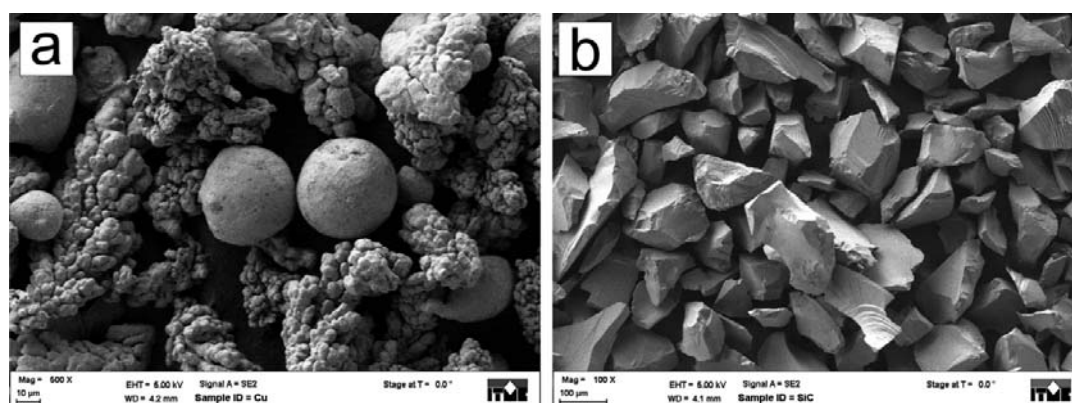


Fig. 1. SEM images of starting materials: (a) copper and (b) silicon carbide.

Five Cu-SiC compositions of powder mixtures, with 5.0, 10.0, 15.0, 20.0 and 25.0 % (in vol.%) of SiC, respectively, were prepared through mechanical mixing process. This process was conducted in air atmosphere using a Pulverisette 6 Fritsch planetary ball mill with a 250 ml vial. The chamber lining and the milling balls ($\varnothing 10$ mm) were made of tungsten carbide with the addition of cobalt. Parameters of the mixing process were as follows: the rotational speed of 200 rpm, the time of mixing of 2 h, ball-to-powder ratio (BPR) of 5:1.

Two different sintering techniques were used for the final densification of powder mixtures: hot pressing (HP) and spark plasma sintering (SPS). The hot pressing process of Cu-SiC powder mixtures was conducted in an Astro Thermal Technology press in the argon atmosphere at 1050 $^{\circ}\text{C}$ under the pressure of 30 MPa. The samples were held at this temperature for 30 min and then cooled naturally to room temperature in the furnace before they were removed. The spark plasma sintering process was conducted in a vacuum atmosphere (5×10^{-5} mbar) using the following parameters: sintering temperature = 950 $^{\circ}\text{C}$, heating rate = 100 $^{\circ}\text{C}/\text{min}$, holding time = 10 min, and pressure = 50 MPa. The powders were sintered in a graphite die and, as the final product, cylindrical samples were obtained (diameter = $\varnothing 10$ mm, height = 5 mm).

Next, the microstructure and thermal properties of the fabricated Cu-SiC composites were examined. The densities of composites were measured with the application of the Archimedes method. The obtained results were compared with theoretical densities estimated from the rule of mixtures.

The microstructure of Cu-SiC composites was examined using scanning electron microscopy (SEM) with the use of Dual-Beam Auriga Zeiss microscope with energy dispersive spectroscopy (EDS) detector (Bruker) with the use of the secondary electron (SE) and backscatter electron (BSE) modes. Further investigations of the interface of SiC-Cu composites were conducted using the transmission electron microscope (TEM) JEOL 1200 operating at an accelerating voltage of 120 kV. To do so, thin lamellas were extracted from interfaces regions by means of a combined scanning electron microscope and gallium focused ion beam mill (FIB) microscope Hitachi NB-5000. A standard cutting procedure was carried out [17]. A tungsten coating was deposited in order to protect the entire exposed surface prior

to FIB milling at the beam current of 0.4 nA, dwell time 0.5 μ s and total time deposition of 6 min. The preliminary milling with the beam current of 20 nA was carried out at the selected sites to expose the lamella. The sample was connected to Omniprobe nanomanipulator by tungsten deposition. Then the sample was separated by the reduction of the remaining lamella support to the parent material followed by the lift out and transfer to a Copper transportation grid and tungsten welded. Final thinning was carried out with the beam current of 0.07-0.34 nA and three degrees of tilting angle to the plane of the specimen. In order to achieve high levels of electron transparency through the lamella for the TEM investigations, samples were thinned to 100-150 nm approximately. It was found that such thickness is suitable for TEM observations [18].

The thermal diffusivity D was measured at room temperature by a laser flash method (LFA 457, Netzsch). The front face of the measured sample was homogeneously heated by an unfocused laser pulse. On the rear face of the sample the temperature increase was measured as a function of time. The mathematical analysis of this temperature/time function allows for the determination of the thermal diffusivity D [19,20]. The thermal diffusivity was measured within the temperature range of 50-300 $^{\circ}$ C.

The specific heat was evaluated for each composition based on the rule of mixtures. The experimental results of the thermal diffusivity and calculated values of the specific heat were used to estimate the thermal conductivity λ . It can be determined from the relation:

$$\lambda = \rho \cdot c_p \cdot D \quad (1)$$

where λ – thermal conductivity in W/mK, ρ – density in g/cm^3 , c_p – specific heat in J/gK, D – diffusivity in mm^2/s .

Experimental results were compared with the modelling based on the rule of mixtures. Voigt and Reuss [21] bounds were applied to calculate the theoretical conductivity for an ideal (non-porous) composite material in a wide range of volume fractions.

3. Results and Discussion

The theoretical density of the obtained composites was defined for the assumed volume contents, using the density of silicon carbide $\rho_{\text{SiC}} = 3.20 \text{ g/cm}^3$ and the density of copper $\rho_{\text{Cu}} = 8.89 \text{ g/cm}^3$. Tab. I shows the densities of the produced hot-pressed Cu-SiC composite materials.

Tab. I Density results of Cu-SiC composite materials.

Method	Chemical composition (vol. %)	Theoretical density (g/cm^3)	Measured density (g/cm^3)	Relative density (%)
Hot pressing (HP)	95Cu-5SiC	8.62	7.63	88.6
	90Cu-10SiC	8.33	7.50	90.0
	85Cu-15SiC	8.05	7.27	90.3
	80Cu-20SiC	7.76	6.81	87.7
	75Cu-25SiC	7.48	6.72	89.9
Spark plasma sintering (SPS)	95Cu-5SiC	8.62	8.48	98.4
	90Cu-10SiC	8.33	8.22	98.7
	85Cu-15SiC	8.05	7.96	98.9
	80Cu-20SiC	7.76	7.71	99.3
	75Cu-25SiC	7.48	7.41	99.1

The hot-pressed Cu-SiC composites demonstrate a worse densification compared to the spark plasma sintered materials. Relative densities oscillate between 88-90 % in all examined cases, despite the application of a higher temperature during hot pressing (1050 °C).

A better densification of composites obtained through the SPS process compared to hot-pressed materials is due to the idea of both processes, namely the manner in which the graphite matrix where the sintered powder is placed is heated up. For the HP method, the heat is transferred to the matrix through convection and radiation. Therefore, the distribution of temperature on the cross-section of the sample is uneven and longer times are required to obtain heterogeneity. As for the SPS method, the set electrical current that passes through graphite plugs, the matrix and the sintered powder (both Cu and SiC are good conductors of electricity) heats the whole system due to the effect of Joule heating. As a result, a local temperature hike on grain-to-grain contact sites is observed (again due to the effect of Joule heating). This has an effect on the speed of the mass transport on the way of evaporation and convection and, at the same time, oxides are removed from the surface of metal particles and the energy of activation of diffusion processes in the powder is decreased, which improves the densification of the material [22,23].

Fig. 2 shows the typical microstructure of Cu-SiC composites after the hot pressing process.

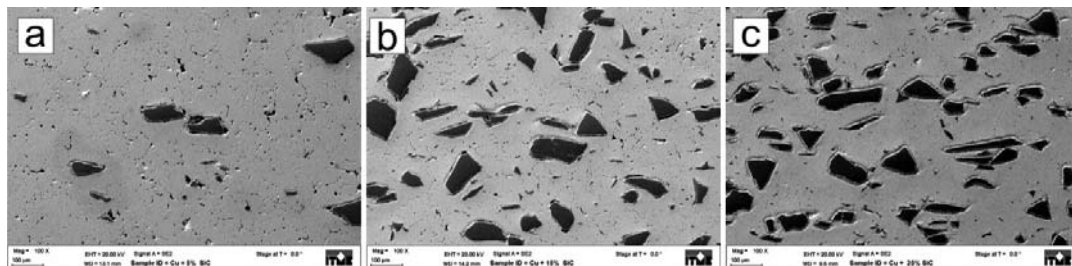


Fig. 2. SEM image of the Cu-SiC composite materials with: a) 5.0 % SiC, b) 15.0 % SiC and c) 25.0 % SiC, obtained through hot pressing method.

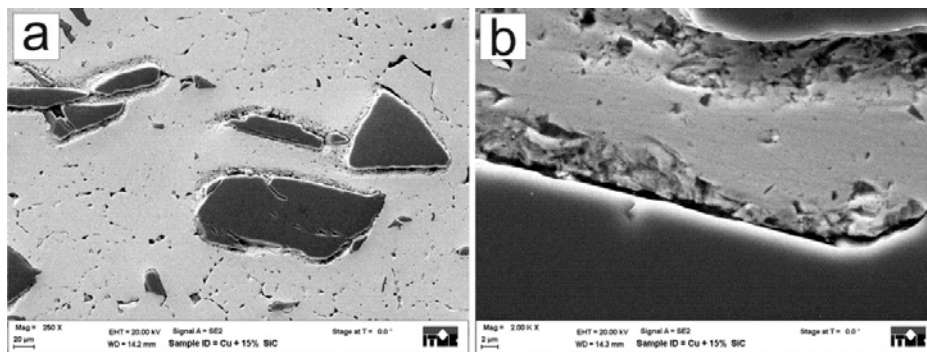


Fig. 3. SEM image of the hot-pressed Cu-15SiC composite structure (a) and ceramic-metal interface (b).

The microstructural studies have shown that the reinforcement phase of the hot-pressed composites has a uniform distribution across the whole of its volume. The aggregation of single SiC grains may be observed locally. Empty spaces (pores) can be observed in places where particular ceramic grains get in direct contact with each other. This results from the lack of possibility to sinter ceramic grains in the conditions of the process (e.g. too low sintering temperature for ceramics). Porosity may be observed also in the areas of the copper matrix of composites where particular copper grains touch one another. A detailed analysis of the microstructure in the ceramic-metal interface shows that this boundary

is highly defective (Fig. 3). SEM analysis revealed that the interface has an irregular shape, which may indicate that some form of reaction occurred during the hot pressing process. A number of pores and the lack of homogeneity between metal and ceramics are observed.

As for spark plasma sintered composites, no differences in the distribution of the ceramic phase in the composite was observed, regardless of the volume fraction of SiC, yet the quality of the obtained materials was significantly higher. The changes involve both the structure of the composite, metal-ceramic interface and the distribution and size of pores. Examples of microstructures of spark plasma sintered Cu-SiC composites are presented in Fig.4.

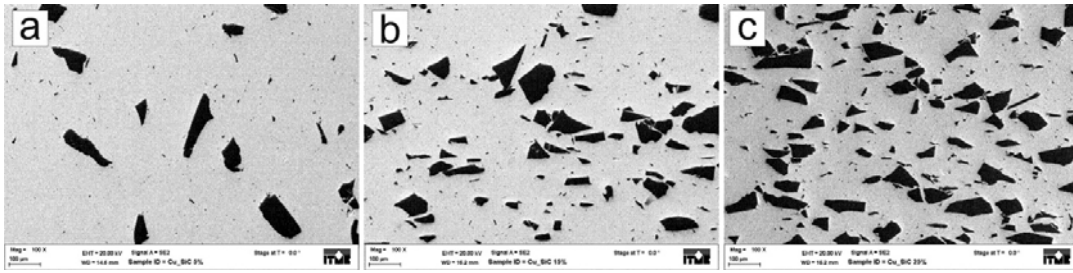


Fig. 4. SEM image of the Cu-SiC composite materials obtained by spark plasma sintering.

Single pores can be observed in the structure of composites and are located mainly in the copper matrix. Their size can be evaluated at approximately 1-2 μm . The distribution of ceramic grains in different directions relative to the pressing axis is generally uniform, which indicates that the composite should exhibit isotropic features.

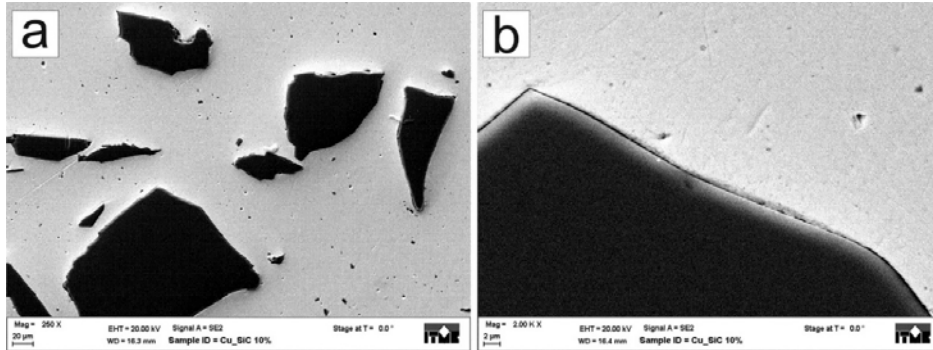


Fig. 5. SEM image of the spark plasma sintered Cu-10SiC composite structure (a) and metal-ceramic interface (b).

SEM imaging did not reveal any additional phases in the interfacial regions which may be formed during the HP or SPS processing. The distribution of chemical elements was investigated by EDS analysis. Chemical element distribution maps of the specimen in the spark plasma sintered composite are presented in Fig.6.

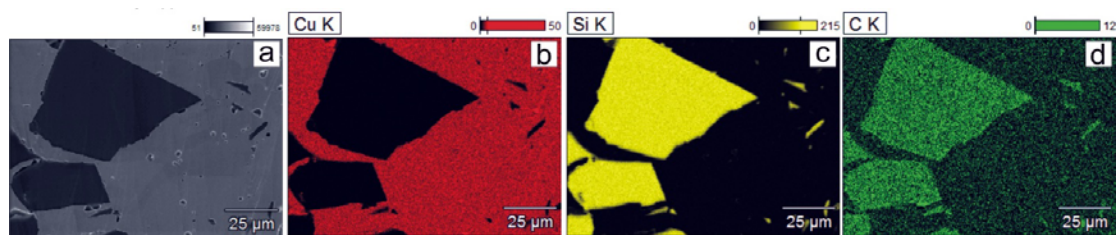


Fig. 6. SEM/EDS maps of surface distribution of elements for Cu-10SiC composite material sintered through the SPS method.

The detailed investigation of Cu-SiC microstructure was performed by TEM studies. The TEM images of thin lamellas of HP and SPS samples are presented in Fig.7a and b, respectively.

The dark areas of both images correspond to the Cu phase and bright ones to SiC. The comparison of these two images allows drawing the following conclusions. First of all, many nanocracks and voids were observed in both interfacial areas between Cu and SiC phases. These defects may be related to the sintering process parameters, which mainly affect the formation of continuous and homogeneous connection between the phases during the hot pressing process. The appearance of interface nanocracks can be also due to thermal residual stresses generated during the cooling process. However, in the sample formed through SPS processing, the number of interfacial defects seems to be smaller, which can be observed on both TEM (Fig.7b) and SEM (Fig. 5) images. The TEM image shows that the Cu-SiC interface in the material obtained through SPS has a more continuous character than the one obtained through HP.

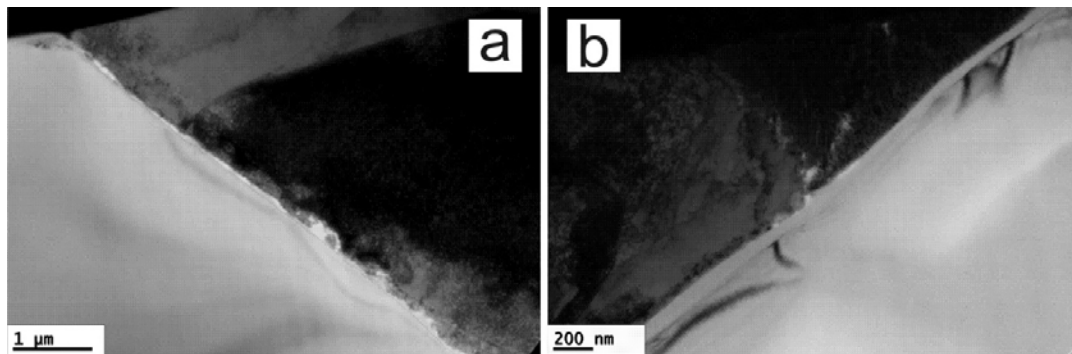


Fig. 7. TEM images of copper-silicon carbide interface.

Moreover, for both samples a thin layer between Cu and SiC phases was found at the interfacial zones, which may indicate that diffusion processes taken place during processing. The diffusional interface, in contrast to adhesive one, is a privileged bonding in view of thermal conductivity. In the order to study the layer, the TEM- EDX analysis was performed on the HP sample. The image of composite interface with the application of a linear distribution of chemical element content is presented in Fig. 8. Green, red and blue lines show the distributions of Si, C and Cu elements, respectively.

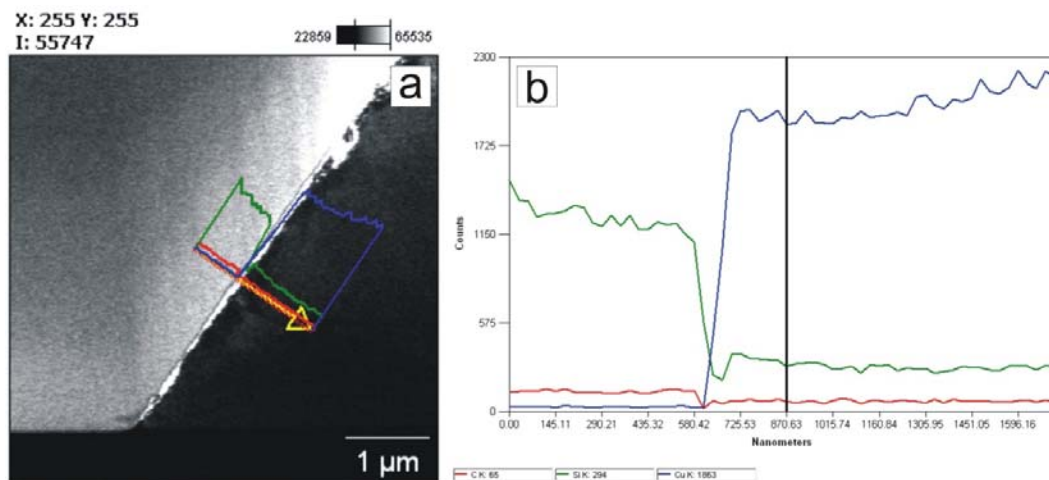


Fig. 8. Linear distribution of elements (Cu, Si, C) across the metal-ceramic interface in Cu-SiC composite after hot pressing.

The results point out that all considered elements occur in the interfacial zone. The thickness of this zone varies between 50 and 150 nm and for SPS samples it seems to be thinner. The observed difference is the result of different heating conditions for the HP and SPS process. Diffusion is a time-consuming process and its range strictly corresponds to the time-temperature regimes. Spark plasma sintering techniques seems to be more efficient processes when the decomposition reaction at an elevated temperature occurs.

Furthermore, the EDX study proves that a part of Si has dissolved in the Cu. This is in agreement of Suganuma et al. [24] who reported that SiC in contact with Cu was decomposed into Si and carbon at about 1100 °C. Other studies also confirm the reaction of Si and C at elevated temperatures [25]. Authors of [26] investigated the kinetics of the formation of Cu_3Si in Cu/Si diffusion couples by differential scanning calorimeter. They found that the Cu_3Si was formed at 450–500 K by either the bulk or grain boundary diffusion mechanism. In addition, Qin et al. [27] postulated the formation of Cu_3Si below 900 °C at the metal/ceramic interface after the decomposition of SiC.

In our investigations no residual carbon layer (as a SiC decomposition product) was identified. Presumably its thickness is very low and did not allow us to confirm its presence with the available techniques. It needs a more detailed analysis with more sophisticated instruments (e.g. SIMS) and it will be our goal in the near future. Thermal properties of both types of Cu-SiC composite materials were examined. Based on the measurement results of thermal diffusivity, thermal conductivity of Cu-SiC composites as a function of temperature was estimated. The obtained results for materials after HP and SPS are presented in Fig. 9a and Fig. 9b, respectively.

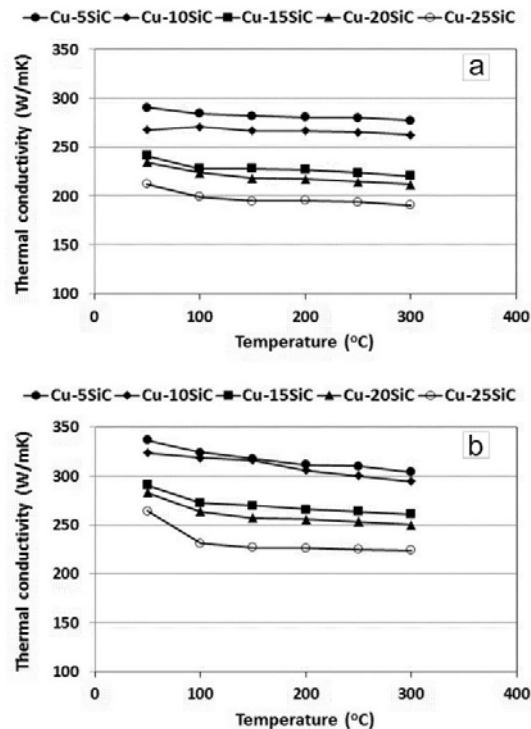


Fig. 9. Thermal conductivity of Cu-SiC composites obtained through: a) hot pressing, b) spark plasma sintering.

A significant difference in the measured values of thermal conductivity for materials obtained through HP and SPS methods was observed. The thermal conductivity, measured at 50 °C, of the composites with a copper matrix reinforced by a variable amount of SiC ranges

between 200 and 300 W/mK. Applying the spark plasma sintering technique allowed to obtain materials with a much higher thermal conductivity for all compositions. In this case thermal conductivity reached the values between 250 and 350 W/mK. The increased amount of ceramic phase in the composite results in the decrease of thermal conductivity. It is an obvious fact depending on the difference in conductivity of both components. It was also found that the thermal conductivity value for all analyzed samples is decreased when the temperature is increased. This phenomenon is typical of the majority of metallic-based materials and is caused by an increased scattering of phonon carriers in the crystal lattice, observed with the raise in temperature.

The obtained results were compared to theoretical values. The roughest estimates of the effective material properties but, at the same time, the most widely used ones, are the Voigt and Reuss bounds. The Voigt upper bound is derived under the assumption of a uniform stress distribution, whereas the Reuss lower bound - under the assumption of a uniform strain distribution. This leads to the solution of elasticity equations, where the stiffness tensor is equal to the average values of the matrix and inclusion stiffness tensors, while the compliance tensor is equal to the average values of the matrix and inclusions compliance tensors. The Voigt and Reuss bounds of the thermal conductivity take the following form [28]:

$$k_V = f_1 k_1 + f_2 k_2$$

$$k_R = \frac{k_1 k_2}{f_1 k_2 + f_2 k_1} \quad (2)$$

For these calculations, thermal conductivity: 380 W/mK – for copper and for 200 W/mK – for SiC were assumed. The calculated results were compared to the experimental measurements for materials obtained through hot pressing and spark plasma sintering (Fig. 10).

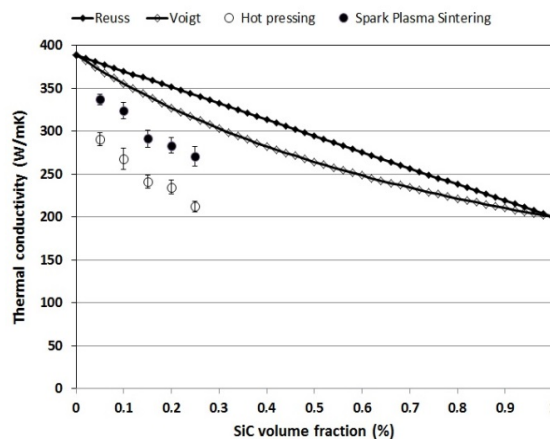


Fig. 10. Theoretical and measured values of the thermal conductivity for Cu-SiC composites.

Following the comparison of the results of a theoretical estimation and real material measurements it can be stated that the measured values of TC are lower than expected. In case of Cu-SiC composite materials sintered through the SPS method the results are lower by approximately 10 %. A much bigger difference (over 20 %) is observed for the hot pressed composites. The reasons of such phenomena should be linked to the structure of materials. The first reason seems to be the residual porosity existing in both types of materials after the consolidation process. As it can be seen in Table 1, the relative density of materials with

different volume content of SiC for each group are as follows: for HP group – 88-90 % and for SPS group – 98-99 %. The heat transfer in the structure with a high amount of porosity is straitened. The pores form a specific barrier, where the heat is dissipated, and the heat flux is limited. Therefore it seems natural - the more pores in the structure, the lower the capacity of thermal conduction. For all examined compositions, the copper matrix creates a continuous structure which is the easiest way to transfer the heat. However, in case where both components of the composite have a good thermal conductivity, the heat transfer across ceramic grains play an important role too. And that is why the quality of the metal-ceramic interface is so significant. Some impurities or discontinuities disrupt the transfer of heat. Additionally, the location of pores at the contact area of particular ceramic grains or at the metal-ceramic grain boundaries are also disadvantageous from the thermal conduction point of view. In case of Cu-SiC materials after hot pressing, we observed many of the aforementioned factors in the microstructure. Especially the interface area was strongly defected. It should be noticed that also silicon dissolved in copper near the ceramic-metal boundary, which affects the thermal conductivity of the matrix. The area where the copper-silicon alloy is formed is much thicker with the use of the HP method. Such a system strictly limited the thermal conductivity of metallic matrix. This process is determined by the conditions of sintering. In case of hot pressing, copper and silicon carbide are subjected to interaction at a high temperature for a much longer time than during spark plasma sintering. The range of the observed changes in the structure of Cu-SiC (SPS) is significantly limited. However, some disadvantageous symptoms were observed too. A possible solution to definitely prevent the decomposition of silicon carbide seems to be the covering of particles by other metals with good thermal properties and nonreactive to SiC like: Ag, Au, Ni, others, which indicate other authors [29, 30].

4. Conclusions

Copper matrix composites with different volume fraction of SiC reinforcement were manufactured by two powder metallurgy techniques. SEM observations confirmed the homogenous distribution of SiC particles in the matrix. A detailed analysis of the composite microstructure revealed some changes in the area of ceramic-metal interface. The presence of some nanocracks or porosity and additionally silicon dissolution process in copper has a negative effect on the thermal properties of Cu-SiC composites. The comparison of two techniques of copper-silicon carbide composites manufacturing has shown that spark plasma sintering provides a better quality of materials, due to shorter interaction times between the components during the heating/cooling cycle.

Acknowledgement

The studies have been carried out within the project entitled The correlation between interface morphology and heat transfer in Cu-SiC composites in function of the form of reinforcement material, financed by the National Science Center within the framework of OPUS Programme (contract ref. no.: 2014/13/B/ST8/04320).

5. References

1. J. Th. M. DeHosson, B. J. Kooi, *Surf. Interface Anal.*, 31(2001) 637.
2. M. W. Finnis, *J. Phys. Condens. Matter.*, 8 (1996) 5811.

3. D. D. L. Chung, Appl. Therm. Eng., 21 (2001) 1593.
4. A. M. Abyzov, M. J. Kruszewski, Ł. Ciupiński, M. Mazurkiewicz, A. Michalski, K. J. Kurzydłowski, Mater. Design, 76 (2015) 97.
5. A. Strojny-Nedza, K. Pietrzak, Sci. Sinter., 47 (2015) 249.
6. G. Celebi Efe, S. Zeytin, C. Bindal, Mater. Design., 36 (2012) 633.
7. M. Chedru, J. Vicens, J. L. Chermant, B. L. Mordike, J. Microsc., 196(2) (1999) 103.
8. M. Chmielewski, W. Weglewski, **Bull. Pol. Acad. Sci.-Te.**, 61(2) (2013) 514,
9. K. M. Lee, D. K. Oh, W. S. Choi, T. Weissgarber, B. Kieback, J. Alloy. Compd., 434-435 (2007) 377.
10. K. Pietrzak, N. Sobczak, M. Chmielewski, M. Homa, A. Gazda, R. Zybala, A. Strojny-Nedza, J. Mater. Eng. Perform, doi: JMEP-15-11-9380.R (2016).
11. G. Sundberg, P. Paul, C. Sung, T. Vasilos, J. Mater. Sci., 40 (2005) 3383.
12. Th. Schubert, B. Trindade, T. Weißgarber, B. Kieback, Mater. Sci. Eng. A, 475 (2008) 39.
13. K. Hyun-Ki, K. Suk Bong, Mater. Sci. and Eng. A, 428 (2006) 336.
14. Z. Lin, Q. Xuan-Hui, D. Bai-Hua, H. Xin-Bo, Q. Ming-Li, R. Shu-Bin, Int J. Miner. Metal. Mater., 16 (3) (2009) 327.
15. J. Grzonka, M. J. Kruszewski, M. Rosiński, Ł. Ciupiński, A. Michalski, K. J. Kurzydłowski, Mater. Charact., 99 (2015) 188.
16. J. Raethel, M. Herrmann, and W. Beckert, Eur. J. Ceram. Soc. 29 (2009) 1419.
17. M. Andrzejczuk, J. Siejka-Kulczyk, M. Lewandowska, K. J. Kurzydłowski, J. Microsc., 237 (3) (2010) 427.
18. S. J. Mee, J.R. Hart, M. Singh, Appl. Clay. Sci., 39 (2008) 72.
19. S. Min, J. Blumm, A. Lindemann, Thermochemica Acta, 455 (2007) 46.
20. M. J. Kruszewski, R. Zybala, M. Chmielewski, B. Adamczyk-Cieślak, A. Michalski, M. Rajska, K. J. Kurzydłowski, J. El. Mater., doi: 10.1007/s11664-015-4037-5 (2016)
21. J. Mihans, S. Ahzi, H. Garmestani, M.A. Khaleel, X. Sun, and B.J. Koeppel, Mater. Design., 30 (2009) 1667.
22. Z. Munir, U. Anselmi-Tamburini, and M. Ohyanagi, J. Mater. Sci. 41 (2006) 763.
23. N. Saheb, Z. Iqbal, A. Khalil, A. S. Hakeem, N. A. Aqeeli, T. Laoui, A. Al-Qutub, and R. Kirchner, J. Nanomater. 2012 (2012) 1
24. K. Sukanuma, K. Nogi, I. J. Jpn. I. Met. Mater., 59 (1995) 1292.
25. H. K. Kang, S.B. Kang, Mater. Sci. Eng. A, 428 (2006) 336.
26. R. R. Chromik, W.K. Neils, E.J. Cotts, J. Appl. Phys., 86 (8) (1999) 4273.
27. C. D. Qin, B. Derby, Brit. Ceram. Trans. J., 90(4) (1991) 124.
28. W. Pabst, E. Gregorova, in "New Developments in Materials Science Research", ed. B.M. Caruta, 77–137, Nova Science Publishers, New York, 2009.
29. H. Ming, Z. Yunlong, T. Lili, S. Lin, G. Jing, D. Peiling, Appl. Surf. Sci., 332 (2015) 720.
30. X. Luo, Y. Yang, Ch. Wang, J. Luo, Ch. Xue, Rare. Metals, 30(4) (2011) 396.

Садржај: Рад представља испитивање колелације између микроструктуре и термичких својстава бакар-силицијум карбидног композита, добијеног топлим пресовањем и спарк плазма синтеровањем. Микроструктурна анализа показује бољу денсификацију у случају композита синтерованог у плазми. ТЕМ испитивања откривају присуство силицијума у области металне матрице у региону близу границе метал-керамика. То је продукт растварања силицијума у бакуру на високим температурама. Гранична површина у композиту Си-SiC је значајно дефектна код узорак добијених топлим пресовањем, што има пресудан значај у термичкој проводљивости материјала.

Кључне речи: композити; силицијум-карбид; гранична површина; спарк плазма синтеровање; термичка проводљивост.

© 2016 Authors. Published by the International Institute for the Science of Sintering. This article is an open access article distributed under the terms and conditions of the Creative Commons — Attribution 4.0 International license (<https://creativecommons.org/licenses/by/4.0/>).

